Open access • Journal Article • DOI:10.1364/OL.40.000597

Perfect vortex beam: Fourier transformation of a Bessel beam. — Source link

Pravin Vaity, Leslie A. Rusch

Institutions: Laval University

Published on: 15 Feb 2015 - Optics Letters (Optical Society of America)

Topics: Bessel beam, Beam diameter, M squared, Laser beam quality and Optical vortex

Perfect vortex beam: Fourier transformation of a Bessel beam

Pravin Vaity and Leslie A. Rusch

OSA Optics Letters, (Volume 40, Number 4) (2015)

Doi: 10.1364/OL.40.000597

https://www.osapublishing.org/ol/abstract.cfm?uri=ol-40-4-597

This article has been accepted for publication in a future issue of this journal, but has not been fully edited. Content may change prior to final publication.
Citation information: DOI 10.1364/OL.40.000597, Optics Letters

Perfect Vortex Beam: Fourier transformation of Bessel Beam

Pravin Vaity* **and Leslie Rusch**

Center for Optics, Photonics and Lasers (COPL), Université Laval, Québec, QC, Canada
**Corresponding author:pravin.vaity.1@ulaval.ca*

Compiled September 22, 2016

We derive a mathematical description of a perfect vortex beam as the Fourier transformation of a Bessel beam. Building on this development, we experimentally generate Bessel-Gauss beams of different orders and Fourier-transform them to form perfect vortex beams. By controlling the radial wave vector of Bessel-Gauss beam, we can control the ring radius of the generated beam. Our theoretical predictions match with the experimental results and also provide an explanation for previous published works. We find the perfect vortex resembles that of an orbital angular momentum (OAM) mode supported in annular profiled waveguides. Our prefect vortex beam generation method can be used to excite OAM modes in an annular core fiber.

OCIS codes: 050.4865, 070.6120, 230.6120.

Optical vortices have wide application in science [1,2]. Their recent application in communication systems, both in free space [3,4] and fiber [5], is a burgeoning area of research. Researchers are attracted towards these beams because they have orbital angular momentum (OAM). However, these conventional vortex beams are limited as their ring diameter depends on the order, or topological charge, l (the number of twist in a wave front per unit wavelength). This property may create problems when coupling multiple OAM beams into a fiber with fixed annular index profile [6-9].

To overcome the limitations of conventional vortex beam, Ostrovsky, et al. [10,11] introduced the concept of a perfect vortex beam: one having ring diameter independent of topological charge. They used a special phase mask, generated from a complex equation, to approximate perfect vortex. The beam they created has undesired extra rings. Another recently published technique for generation of perfect vortex beams uses an axicon [12]. A beam with fixed ring diameter, proportional to the axicon parameter, can be achieved at any vortex order. This technique, however, require the axicon be replaced and the setup re-aligned to achieve different ring diameter.

To simplify generation and overcome the above mentioned drawbacks, we demonstrate a new technique to form a perfect vortex beam with controllable ring radius using the Fourier transform property of a Bessel beam. The derivation of this transform is obtained theoretically and used to generate a perfect vortex beam. We implement our technique by using spatial light modulator (SLM). The new phase mask for the SLM is designed by combining an axicon and a spiral phase function to form a Bessel-Gauss (BG) beam. Then this BG beam is optical Fourier-transformed through a simple lens. By controlling the axicon parameter in creating the phase mask, one can control the BG beam's radial wave vector and consequently ring radius of the perfect vortex. We also studied detection of these beams or their conversion back to Gaussian beam. The application of perfect vortex beam for excitation of OAM mode in an annular waveguide is discussed at the end.

Consider an ideal Bessel beam equation in the cylindrical coordinate system (ρ, ϕ, z) with unit amplitude [13],

$$E(\rho, \phi, z) = J_l(k_r \rho)\exp(il\phi + ik_z z), \tag{1}$$

where J_l is an l^{th} order Bessel function of first kind. k_r and k_z are the radial and longitudinal wave vectors, with the wave vector $k = \sqrt{k_r^2 + k_z^2} = \frac{2\pi}{\lambda}$.

A simple lens can act as an optical Fourier transformer. This transformation for any arbitrary field $E(\rho, \phi)$ into $E(r, \theta)$ can be written mathematically in cylindrical coordinates as [14],

$$E(r,\theta) = \frac{k}{i2\pi f}\int_0^\infty \int_0^{2\pi} E(\rho,\phi)\rho d\rho d\phi \exp\left(\frac{-ik}{f}\rho r\cos(\theta-\phi)\right), \tag{2}$$

where f is the focal length of the lens. After substituting Eq. (1) into (2), the Fourier transform of the Bessel beam is,

$$E(r,\theta) = \frac{k}{f} i^{l-1}\exp(il\theta)\int_0^\infty J_l(k_r\rho)J_l(kr\rho/f)\rho d\rho. \tag{3}$$

Using the orthogonality of Bessel functions, the above equation can be reduced to the Dirac delta function $\delta(r)$, as,

$$E(r,\theta) = \frac{i^{l-1}}{k_r}\delta(r - r_r)\exp(il\theta). \tag{4}$$

The above equation represents the complex field amplitude of an ideal perfect vortex beam having topological charge l and ring radius $r_r = k_r f/k$. The same equation is considered in the reference [10]. As the formation of a Dirac delta field in an experiment is difficult, the above

This article has been accepted for publication in a future issue of this journal, but has not been fully edited. Content may change prior to final publication.
Citation information: DOI 10.1364/OL.40.000597, Optics Letters

equation is reduced to a finite-sum approximation in the same reference. The simulated intensity profile plotted from such an approximation has a bright center ring, with extra undesired lateral rings. The center ring is the perfect vortex while the others are present due to the truncated sum approximation.

While experimental realization of an ideal Bessel beam is not possible, one can always form a Bessel-Gauss beam experimentally with complex field amplitude [15],

$$E(\rho,\phi) = J_l(k_r\rho)\exp(il\phi)\exp\left(-\frac{\rho^2}{w_g^2}\right), \tag{5}$$

where w_g is the beam waist of the Gaussian beam which is used to confine the Bessel beam. Again, the Fourier transform of the above equation is derived by substituting it into Eq. (2),

$$E(r,\theta) = \frac{k}{f}i^{l-1}\exp(il\theta)\int_0^\infty J_l(k_r\rho)J_l(kr\rho/f) \exp\left(-\frac{\rho^2}{w_g^2}\right)\rho d\rho. \tag{6}$$

Using standard integral and Bessel function identity [16], one can write Eq. (6) as,

$$E(r,\theta) = i^{l-1}\frac{w_g}{w_0}\exp(il\theta)\exp\left(-\frac{r^2+r_r^2}{w_0^2}\right)I_l\left(\frac{2r_r r}{w_0^2}\right). \tag{7}$$

The above equation represents the field amplitude of a perfect vortex having ring width and radius equal to $2w_0$ and r_r respectively. Here, I_l is an l^{th} order modified Bessel function of first kind. The Gaussian beam waist at the focus is $w_0(=\frac{2f}{kw_g})$. Equation (7) is the combination of two functions: a modified Bessel function and a Gaussian function. Since I_l grows exponentially, both function intersect at $r = r_r$ to form a ring. As the slope of the curve of I_l slightly decreases with l, the ring radius shifts by a small value. One can always control decrease experimentally by changing the axicon parameter.

As the Fourier plane lies at the focus of the lens, w_0 is small. For large r_r, one can approximate I_l as

$$I_l(\frac{2r_r r}{w_0^2}) \sim \exp(\frac{2r_r r}{w_0^2}). \tag{8}$$

So that the Eq. (7) can be reduced to

$$E(r,\theta) = \frac{w_g i^{l-1}}{w_0}\exp(il\theta)\exp\left(-\frac{(r-r_r)^2}{w_0^2}\right). \tag{9}$$

The above expression is similar to the expression mentioned in the reference [12]. This equation can be reduced to Eq. (4) for small w_0 or for $w_0 = 0$. Overall, Eq. (7) is the true representation of the complex field amplitude of perfect vortex beam.

For the sake of simplicity, one can write Eq. (7) in the following form having constant amplitude A_0 at $z = 0$ plane,

$$E(r_1,\theta_1) = A_0\exp(il\theta_1)\exp\left(-\frac{r_1^2}{w_0^2}\right)I_l\left(\frac{2r_r r_1}{w_0^2}\right). \tag{10}$$

Now, consider the Fresnel diffraction formula for study of free space propagation of perfect vortex beam [14].

$$E(r_2,\theta_2,z) = \frac{k}{i2\pi z}\exp(ikz)\int_0^\infty\int_0^{2\pi} E(r_1,\theta_1)r_1 dr_1 d\theta_1 \exp\left(\frac{ik}{2z}(r_1^2+r_2^2-2r_1r_2\cos(\theta_2-\theta_1))\right). \tag{11}$$

After putting Eq. (10) into Eq.(11), we obtain

$$E(r_2,\theta_2,z) = A_0\frac{w_0}{w}(-1)^l\exp(i\psi+il\theta_2+ikz) \exp\left(\frac{ik}{2R}(r_2^2+r_r^2)\right)\exp\left(\frac{-1}{w^2}(r_2^2-(\frac{r_r z}{z_r})^2)\right) I_l\left(\frac{2r_r r_2\exp(i\psi)}{w_0 w}\right). \tag{12}$$

Here, w is the beam radius at z, R is the radius of curvature and ψ is the Gouy phase shift of the Gaussian beam. The beam parameters w, R, and ψ are related to the waist spot size w_0 and the Rayleigh range $z_r = kw_0^2/2$ by

$$w = w_0\sqrt{1+(\frac{z}{z_r})^2}, R = z+\frac{z_r^2}{z}, \psi = \arctan(\frac{z}{z_r}). \tag{13}$$

From equation (12), we observe the beam profile has a Gaussian nature. It does not show any non-diffraction property.

To study experimental generation of perfect vortex beams, we use our theoretical finding that the Fourier transform of a BG beam is an annular-shaped perfect vortex having finite ring width and diameter. The BG beam can be created using an axicon. The generation of a perfect vortex is divided into two stages. The first stage generates the BG beam with controllable radial wave vector k_r and topological charge l. The second stage converts this beam to a perfect vortex of topological charge l having ring radius r_r using the Fourier transform property of a simple lens.

We start with generation of BG beam having different value of k_r and l using a phase mask as shown in Fig. 1. This phase mask is formed by plotting an argument of function $\exp(iar + il\theta)$, which is the combination of an axicon function and a spiral function. Here, a is the axicon parameter. The BG beam generated from such a phase mask have radial and longitudinal wave vector which can be calculated from the axicon parameter ($a = k\tan^{-1}(k_r/k_z) = k\sin^{-1}(k_r/k) = k\cos^{-1}(k_z/k)$). The first zero of the zeroth order BG beam is equal to 2.405 times the inverse of k_r [13].

We next consider the lens that Fourier-transforms the BG beam to form perfect vortex beam. By controlling

This article has been accepted for publication in a future issue of this journal, but has not been fully edited. Content may change prior to final publication.
Citation information: DOI 10.1364/OL.40.000597, Optics Letters

the input beam radius w_g (used to form the BG beam), one can control the Gaussian beam waist w_0 at the focus, which is actually half the ring-width of the perfect vortex. The ring radius r_r of a perfect vortex depends on radial vector k_r, which can be controlled by an axicon parameter via the phase mask. At the same time, the same phase mask gives a vortex nature with topological charge l to the ring beam.

Figure 1 shows the experimental setup for generation of a perfect vortex beam with different topological charges. The beam from a semiconductor laser (Cobrite DX1 at wavelength, 1550 nm) with a single mode fiber patch cord is collimated by a collimating lens to form a free space beam of 2 mm diameter. The SLM (PLUTO, phase only spatial light modulator from Holoeye) screen having phase mask is illuminated by a collimated beam to form a BG beam of different topological charge and radial vector. The field distribution of the diffracted beam from the phase mask is Fourier transformed by using a physical lens of focal length 50 cm. The Fourier transformed field forms a perfect vortex beam at the focus point. The ring dynamics is studied by recording the intensity profile through a CCD camera (Spiricon, SP620U-1550).

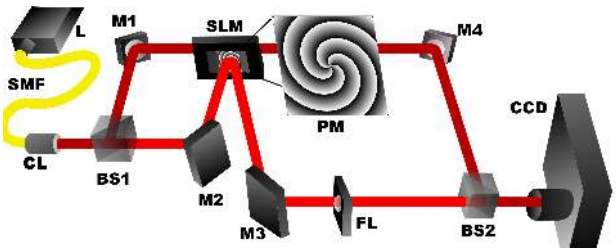

Fig. 1. Experimental setup: L, laser; SMF, single mode fiber; CL, collimating lens, M1, M2, M3, M4, mirrors; BS1, BS2, beam splitters; SLM, spatial light modulator; PM, phase mask; FL, Fourier lens; CCD, CCD camera.

The generation of zeroth and fourth order BG beams for different values of axicon parameter is shown in Fig. 2. The intensity profile of these beams is recorded by a CCD camera after the SLM. As expected, the full width half maximum (FWHM) of the zeroth order BG's center lobe increases with decreasing axicon parameter. Since $k_r = 2.405/B_0$ (where B_0 is the first zero of zeroth order Bessel beam), one can calculate k_r experimentally and verify with the axicon parameter. The experimental results are verified with the theoretical plot obtained from Eq. (5). There is only a small discrepancy between experimental and theoretical results. Due to saturation of the intensity of main lobe in the experiment, we could not record all rings of the beam. As we increase the exposure time, the contrast between the central rings and the lateral ones becomes so small that they could not resolve. Note that the number of rings of a BG beam is practically limited by resolution and aperture size of SLM.

We next Fourier-transform the BG beams to form perfect vortex beams. These transformations are shown in Fig. 3 for different values of a. The ring radius of the perfect vortex decreases with decreasing a, irrespective of its topological charge. For $a = 0$, it forms a conventional optical vortex. For verification and comparison, the theoretical results obtained from Eq. (7) are also shown in the same figure. The measurements match well with theory. As predicted in theory, the ring radius remains constant for all orders, or topological charges. However, as the order of a perfect vortex increases by one in the experiment, the ring radius shifts by 0.04 times of ring width which can be corrected via the axicon parameter.

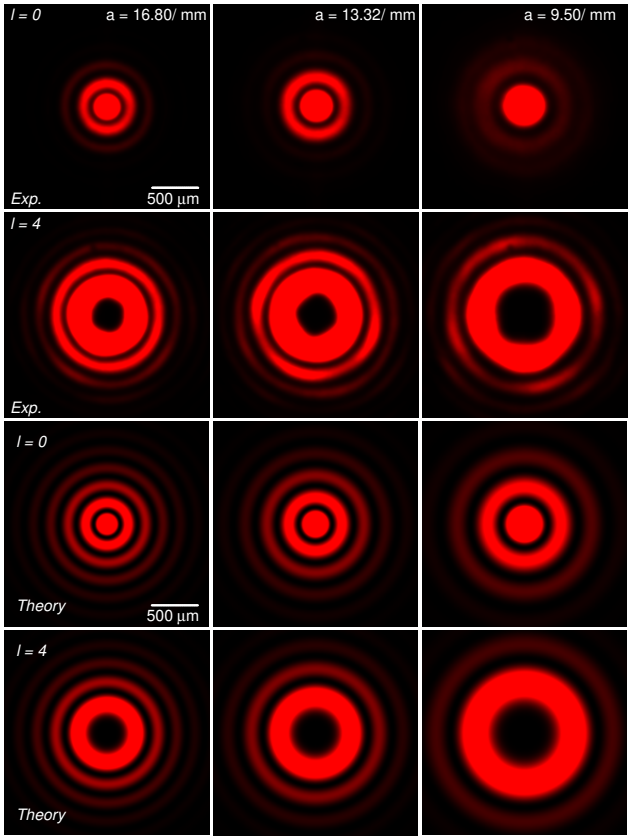

Fig. 2. Generation of zeroth and fourth order Bessel-Gauss beams

The vortex nature of the ring beam generated from Fourier transform of the BG beam is verified through interferometry. Figure 4 shows the interference pattern obtained by interfering a perfect vortex and Gaussian beam. We observe a spiral fringe pattern, which confirms the presence of OAM in the perfect vortex beam. The number of spirals represents the order or topological charge of the perfect vortex, and its direction of rotation decides the sign.

Unlike its Fourier pair, this ring beam diffracts in both direction towards the center, as well as away from the center following a Gaussian divergence law. If $r_r >> w_0$, the ring beam maintains its annular shape; otherwise it forms an Airy pattern after a finite distance of propagation.

This article has been accepted for publication in a future issue of this journal, but has not been fully edited. Content may change prior to final publication.
Citation information: DOI 10.1364/OL.40.000597, Optics Letters

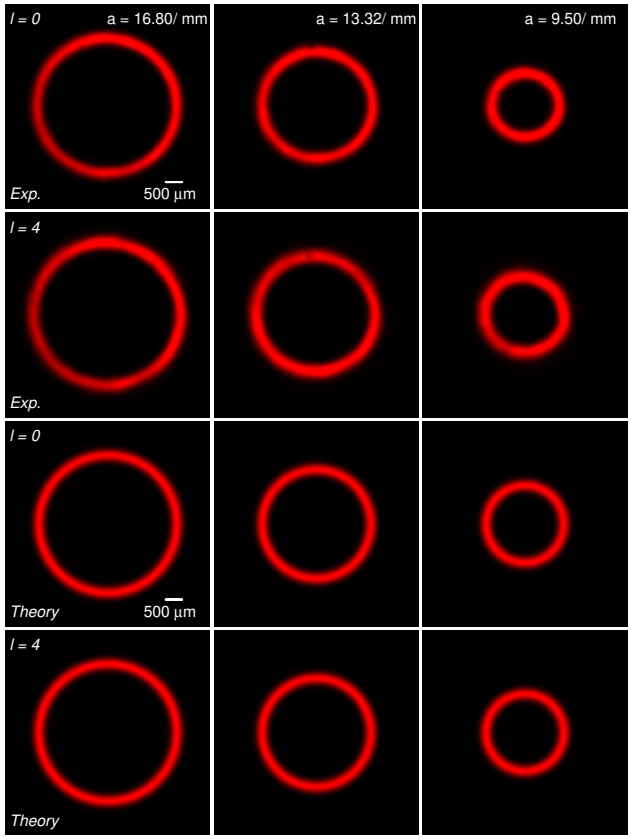

Fig. 3. Generation of perfect vortex beams through Fourier transformation of Bessel-Gauss beams

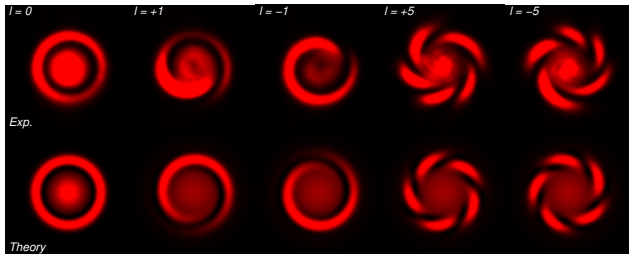

Fig. 4. Interference pattern of perfect vortex beam and Gaussian beam.

In many applications like fiber based communications [3-5] and quantum computing [2], it is necessary to convert a vortex beam to a Gaussian beam for detection. This is easily possible with a conventional vortex beam. In the case of a perfect vortex, however, it is complex. The perfect vortex never converts back to the Gaussian by passing through a spiral phase mask or spiral + axicon phase mask. We must convert the perfect vortex to BG beam. After then passing through a spiral + axicon phase mask, the BG beam becomes Gaussian. The phase mask for generation and detection should be the same but with an opposite sign of spiral.

Since the perfect vortices have the same profile as OAM modes present in the annular shaped waveguides, they can be used to excite OAM modes in such waveguides [6-9]. We used these beams to study OAM mode excitation in an air-core fiber [17]. The verification of 36 OAM modes was only possible by exploiting perfect vortices. Due to the controllable ring width, radius and topological charge, we could match mode field diameter of the OAM modes of the fiber with perfect vortices. We expect to be alike to form radially or azimuthally polarized perfect vortex beams by using the same annular core fiber.

In conclusion, we have studied generation of perfect vortex via Fourier transformation of BG beams. Our theory is validated with experimental results, as well as previously published results. The vector counterpart of perfect vortices may be the solution of annular-shaped waveguides. These beams have the potential for excitation of OAM modes in ring fibers, which are under development in OAM based fiber data communication systems.

References

1. M. J. Padgett and L. Allen, Contemporary Phys., **41,** 275 (2000).
2. G. Molina-Terriza, J. P. Torres, and L. Torner, Nature Phys., **3,** 305 (2007).
3. I. B. Djordjevic and M. Arabaci, Opt. Express,**18,**24722 (2010).
4. J. Wang, J. Yang, I. M. Fazal, N. Ahmed, Y. Yan, H. Huang, Y. Ren, Y. Yue, S. Dolinar, M. Tur and A. E. Willner, Nat. Photonics, **6,** 488 (2012).
5. N. Bozinovic, Y. Yue, Y. Ren, M. Tur, P. Kristensen, H. Huang, A. E. Willner, and S. Ramachandran, Science **340,** 1545 (2013).
6. Y. Yue, Y. Yan, N. Ahmed, Y. Jeng-Yuan, Z. Lin, R. Yongxiong, H. Hao, K. M. Birnbaum, B. I. Erkmen, S. Dolinar, M. Tur, A. E. Willner, Photonics J., IEEE, **5,** 7101007 (2013).
7. P. Gregg, P. Kristensen, S. Golowich, J. Olsen, P. Steinvurzel, and S. Ramachandran, Proc. CLEO, CTu2K.2, San Jose (2013).
8. C. Brunet, B. Ung, Y. Messaddeq, S. LaRochelle, E. Bernier, and L. Rusch, Proc. OFC, Th2A.24, San Francisco (2014).
9. H. Yan, E. Zhang, B. Zhao, and K. Duan, Opt. Express **20,** 17904 (2012).
10. A. S. Ostrovsky, C. Rickenstorff-Parrao, and V. Arrizn, Opt. Lett. **38,** 534 (2013).
11. J. García-García, C. Rickenstorff-Parrao, R. Ramos-García, V. Arrizón and A. S. Ostrovsky, Opt. Lett. **39,** 5305-5308 (2014).
12. M. Chen, M. Mazilu, Y. Arita, E. M. Wright, and K. Dholakia, Opt. Lett. **38,** 4919 (2013).
13. D. McGloin and K. Dholakia, Contemporary Phys., **46,** 15 (2005).
14. J. Goodman, *Introduction to Fourier Optics* (Roberts and Company, Greenwood Village, 2004).
15. F. Gori, G. Guattari, and C. Padovani, Opt. Commun. **64,** 491 (1987).
16. I. S. Gradshteyn and I. M. Ryzhik, *Table of Integral, Series, and Products* (Acdemic Press, San diego, 2001)
17. C. Brunet, P. Vaity, Y. Messaddeq, S. LaRochelle, and L. A. Rusch, Opt. Express **22,** 26117-26127 (2014).